RAA 2015 Vol. **15** No. **7**, 1045–1056 doi: 10.1088/1674–4527/15/7/012
http://www.raa-journal.org *http://www.iop.org/journals/raa*

***R**esearch in*
***A**stronomy and*
***A**strophysics*

Galactic coordinate system based on multi-wavelength catalogs *

Ping-Jie Ding, Zi Zhu and Jia-Cheng Liu

School of Astronomy and Space Science, Nanjing University, Nanjing 210093, China;
dingpjlcj@163.com
Key Laboratory of Modern Astronomy and Astrophysics (Nanjing University), Ministry of Education, Nanjing 210093, China

Received 2014 November 7; accepted 2014 December 12

Abstract The currently used Galactic coordinate system (GalCS) is based on the FK5 system at J2000.0, which was transformed from the FK4 system at B1950.0. The limitations and misunderstandings related to this transformed GalCS can be avoided by defining a new GalCS that is directly connected to the International Celestial Reference System (ICRS). With more data at various wavelengths released by large survey programs, a more appropriate GalCS consistent with features associated with the Milky Way can be established. We try to find the best orientation of the GalCS using data from two all-sky surveys, AKARI and WISE, at six wavelengths between 3.4 μm and 90 μm, and synthesize results obtained at various wavelengths to define an improved GalCS in the framework of the ICRS. The revised GalCS parameters for defining the new GalCS in the ICRS are summarized as: $\alpha^{\rm p} = 192.777^\circ$, $\delta^{\rm p} = 26.9298^\circ$, for the equatorial coordinates of the north Galactic pole and $\theta = 122.95017^\circ$ for the position angle of the Galactic center. As one of the Galactic substructures, the Galactic warp exhibits different forms in different GalCSs that are constructed with various data and methods, which shows the importance of re-defining the GalCS by the relative commission of the International Astronomical Union that can lead to a better understanding of Galactic structure and kinematics.

Key words: astrometry — catalogs — Galaxy: general — reference system

1 INTRODUCTION

The Galactic coordinate system (hereafter GalCS) is a practical coordinate system for studies of Galactic structure, kinematics and dynamics. The current GalCS adopted by the Hipparcos team is related to the J2000.0 FK5-based reference system (Murray 1989) which was transformed from its original IAU 1958 definition based on the FK4 reference system (Blaauw et al. 1960). Liu et al. (2011a) found that this transformed coordinate system is not ideal for this kind of application and using it can lead to misunderstandings. So, a new GalCS directly related to the International Celestial Reference System (ICRS) is necessary. More recently, Liu et al. (2011b, hereafter L11b) updated the three parameters that define the directions of axes for the GalCS in the equatorial system, namely $\alpha^{\rm p}$, $\delta^{\rm p}$ and θ (see Fig. 1), with Sgr A* being the direction of the Galactic center (GC), by including data from the Two Micron All Sky Survey (2MASS) in the near-infrared band and SPECFIND v2.0

∗ Supported by the National Natural Science Foundation of China.

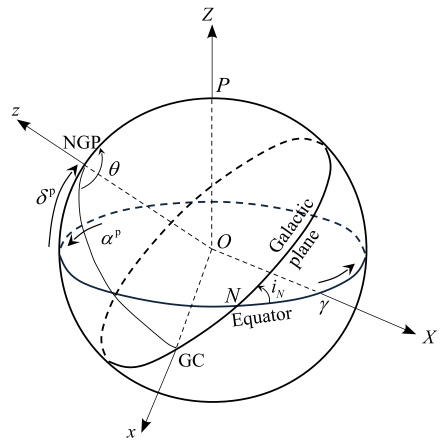

Fig. 1 The definition of the GalCS $[x,\ y,\ z]$ in the ICRS $[X,\ Y,\ Z]$, where NGP is the north Galactic pole and GC is the direction of the Galactic center. The orientation of the GalCS is defined by three parameters, $\alpha^{\rm p}$, $\delta^{\rm p}$ and θ. $i_{\rm N}$ is the inclination of the $x-y$ plane of the GalCS with respect to the equator.

in the radio band. The deviations in terms of the inclination of the Galactic plane with respect to the equator between the new and J2000.0 systems are 0.4° and 0.6° for 2MASS and SPECFIND v2.0 results, respectively (L11b).

With the GalCS parameters $(\alpha^{\rm p}, \delta^{\rm p}, \theta)$, the transformation matrix $\mathcal{N}$ from the equatorial to the GalCS can be written as

$$\mathcal{N} = \mathcal{R}_3\left(90^\circ - \theta\right)\mathcal{R}_1\left(90^\circ - \delta^{\rm p}\right)\mathcal{R}_3\left(90^\circ + \alpha^{\rm p}\right)\ . \tag{1}$$

New transformation matrixes corresponding to near-infrared and radio catalogs have been given by L11b to define revised GalCS in the ICRS. However, there remains room for improvement in establishing a more proper GalCS. First, only catalogs in the two bands were used to obtain the parameters for the GalCS. We note that the GalCS should reveal the feature at multiple wavelengths for the Milky Way, therefore we need catalogs at more wavelengths, such as mid-infrared and far-infrared bands, to obtain a comprehensive result. Second, the methods used to fit the basic plane of the GalCS in L11b are not sufficient to find an ideal basic plane and need to be improved. Some problems, e.g. the southward bias in the basic plane in the direction of GC, should be discussed. We also note that an explicit definition and recommendation for the new GalCS was not given by L11b.

In this work, we use catalogs from the AKARI infrared all-sky survey (Murakami et al. 2007) and the Wide-field Infrared Survey Explorer (WISE) (Wright et al. 2010) All-Sky Release Source Catalog to calculate the GalCS parameters. In Section 2 we describe the catalogs used to fit the position of the basic plane and sample selection according to properties of the data. In Section 3 we introduce the methods for fitting the GalCS parameters: the methods are based on the work of L11b with several improvements. The GalCS parameters at different wavelengths and the results to define a new GalCS are summarized. In Section 4, we present and compare the form of the Galactic warp, one of the notable structures in the Milky Way, in various GalCSs constructed by surveys at different wavelengths. Finally, in Section 5 we discuss several observational effects on the new GalCS and the precision of our results. The final conclusion is also summarized.

2 DATA

As described in L11b, a well-defined GalCS should coincide with the features of the Milky Way. An optimal GalCS means that the distribution of the Galactic sources on the celestial sphere is symmetric about the basic plane (i.e. x-y plane) in the GalCS.

In order to obtain the distribution of Galactic sources, we need to select data covering the Milky Way belt almost completely and homogeneously. It should be noted that interstellar extinction prevents us from obtaining a complete distribution of stars in the optical band. Thus large infrared catalogs are the most suitable data to find the position of the basic plane because the effect of extinction in a band with long wavelengths is relatively weak. In this work, we use catalogs from the AKARI infrared all-sky survey (Murakami et al. 2007) and catalogs from WISE (Wright et al. 2010) to carry out the following computations.

2.1 AKARI

There are two catalogs from the AKARI survey that we include in the analysis: AKARI/IRC (the infrared camera) mid-infrared catalogue (Onaka et al. 2007; Ishihara et al. 2010) and AKARI/FIS All-Sky Survey Bright Source Catalogue Version 1.0 (Kawada et al. 2007). The mid-infrared catalog provides sources in two broad bands centered at 9 μm and 18 μm, respectively. The survey covers the whole sky uniformly. The number of sources in the 9 μm band is 844 649, and the limiting flux is 50 mJy. For the 18 μm band, the number of sources is 194 551, with a limiting flux of 120 mJy (Ishihara et al. 2010). The sample size of the data at 18 μm is not large enough to find a credible basic plane. For this reason we only use the 9 μm-band data from the mid-infrared catalog.

We note that sources near the Sun trace some local structures such as the Gould Belt (Westin 1985) and the warp (Miyamoto et al. 1988), which can lead to bias when we try to find a reliable basic plane that is the closest fit to the main features of the Milky Way projected on the celestial sphere. Therefore we rejected sources near the Sun by removing sources with fluxes larger than 45 Jy because their parallaxes were not available in the catalogs. On the other hand, extragalactic sources with low fluxes or which are separate from the Milky Way (e.g. the Large and Small Magellanic Clouds) may appear in the catalog. Therefore we deleted sources with fluxes below 0.101 Jy and only retained data within the Galactic latitudes $|b| < 15^\circ$ (hereafter simply called "latitudes") to avoid these sources. The upper panel of Figure 2 shows the distribution of selected sources observed at the 9 μm band for the mid-infrared catalog in the J2000.0 GalCS.

The AKARI/FIS all-sky survey covered four bands, centered at 65 μm, 90 μm, 140 μm and 160 μm, respectively (Kawada et al. 2007). We use 90 μm data because a sufficient number of sources are only available for that wavelength. The flux range is restricted between 0.46 Jy and 120 Jy for the same reasons described for selecting 9 μm data. Note that the distribution of objects in the 90 μm band is not very uniform, so we only retain data within $|b| < 6^\circ$. The lower panel of Figure 2 is the distribution of sources observed at 90 μm for the far-infrared catalog in the J2000.0 GalCS. From both plots in Figure 2, we can clearly see the Milky Way projected on the celestial sphere. This kind of distribution of stars will be used to find the best position of the basic plane in the following sections.

2.2 WISE

The WISE all-sky catalog contains positions and four-band (centered at 3.4 μm, 4.6 μm, 12 μm, 22 μm respectively) information on photometry, such as magnitudes, reliability indices and quality flags, for 563 921 584 objects (Wright et al. 2010), as well as information on the associated sources in the 2MASS Point Source Catalog (PSC). It provides us with a lot of data at four additional wavelengths for calculating the GalCS.

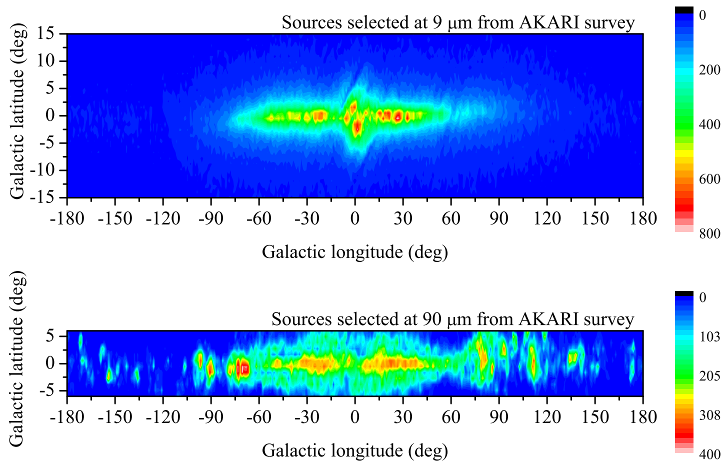

Fig. 2 The distribution of point sources selected from 9 μm (*upper panel*) and 90 μm (*lower panel*) observations of AKARI. The latitudes of sources at 9 μm are between $\pm 15^\circ$ and the fluxes are in the range from 0.101 Jy to 45 Jy. Sources at 90 μm are restricted to have latitude within $\pm 6^\circ$, with fluxes between 0.46 Jy and 120 Jy.

It should be noted that WISE data are not restricted to point-like objects such as stars. The objects may be contaminated or biased owing to probable proximity to an image artifact. Therefore, we used measurement quality and source reliability indices provided by the WISE catalog to select point-like sources for calculation.

We need to reject bright sources (i.e. sources with low magnitude) in the WISE catalog like what we did for AKARI data. But in this procedure, many intrinsically bright stars near the GC but far from the Sun are also simultaneously rejected. The detection rate away from the Galactic disk in the WISE survey is so deep that the source density far from the GC is much larger than that near the GC because we have discarded too many bright stars near the GC. Since these stars are crucial for finding a proper basic plane with our methods, we have to retain them by setting a lower limit on magnitude compared to that for AKARI. Through a series of tests, we finally determined the magnitude ranges of selected WISE sources, which are defined by $10 < m_{3.4\mu\mathrm{m}} < 14.8$, $9 < m_{4.6\mu\mathrm{m}} < 14.5$, $8.5 < m_{12\mu\mathrm{m}} < 12.4$ and $5.5 < m_{22\mu\mathrm{m}} < 8.8$.

Figures 3 and 4 show the distribution of selected sources in the four bands from the WISE all-sky catalog. We also set a limit on the latitudes in each band like we did when analyzing the AKARI catalogs. We retain the data with $|b| < 25^\circ$ in the 3.4 μm band and $|b| < 20^\circ$ in the 4.6 μm band. Unfortunately, the shapes of the Milky Way in the 12 μm band and the 22 μm band are not clearly visible as shown in Figure 4, so we have to narrow the range of longitude and latitude to keep the data as homogeneous as possible. In the direction of longitude, we only retain sources inside the longitude range from -60° to 60° and define a much smaller range of latitude restricted to $|b| < 4^\circ$ for 12 μm and $|b| < 3^\circ$ for 22 μm.

3 METHODS AND RESULTS

In this section we calculate the three parameters $(\alpha^{\mathrm{P}}, \delta^{\mathrm{P}}, \theta)$ that describe the GalCS orientation in the equatorial coordinate system, with improved L11b methods. We can obtain the direction of the north Galactic pole (NGP), the z-axis, by fitting the equation for the position of the basic plane of GalCS to the distribution of chosen data. We can also adopt the direction of GC, i.e. the direction of

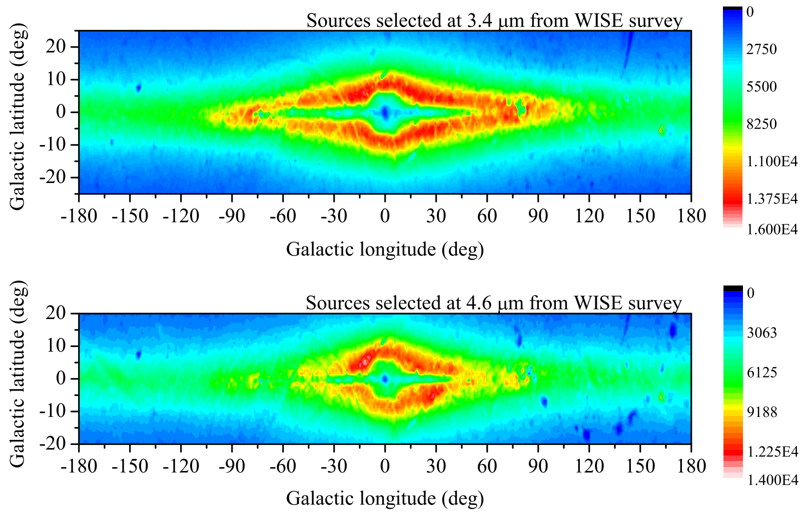

Fig. 3 The distribution of point sources selected at 3.4 μm (*top panel*) and 4.6 μm (*bottom panel*) from the WISE all-sky catalog. The sources at 3.4 μm are in the magnitude range $10 < m_{3.4\mu m} < 14.8$ between -25° to 25° in latitude. The sources at 4.6 μm are in the magnitude range $9 < m_{4.6\mu m} < 14.5$ between -20° and 20° in latitude.

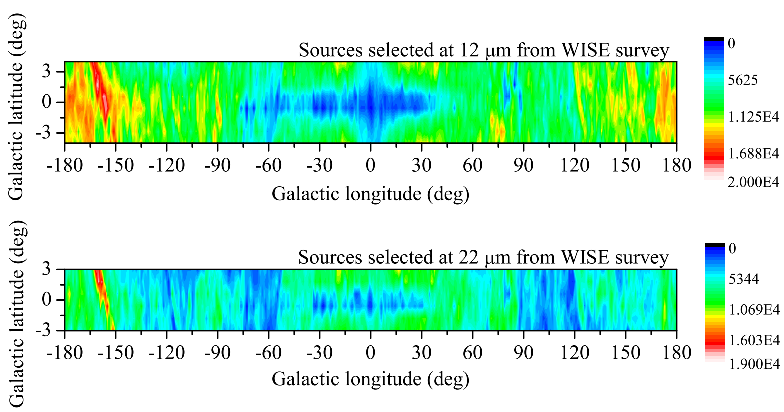

Fig. 4 The distribution of point sources selected at 12 μm (*top panel*) and 22 μm (*bottom panel*) from the WISE all-sky catalog. The sources at 12 μm are in the magnitude range $8.5 < m_{12\mu m} < 12.4$ between -4° and 4° in latitude. The sources at 22 μm are in the magnitude range $5.5 < m_{22\mu m} < 8.8$ between -3° to 3° in latitude.

the x-axis in the GalCS, using results from direct observations of Sgr A*. Because these two axes are actually based on different kinds of observations, the directions of the z-axis and x-axis obtained independently cannot be orthogonal. So, we can only fix one of these axes (expressed by two of the three parameters) preferentially and then determine the third parameter (usually a position angle θ or η, see following subsections) to define the orientation of the other axis. This procedure will ensure the orthogonality of the new GalCS.

In this work we used two methods to find the orientation of the GalCS. The first method is to fix the z-axis of the GalCS from the least-squares (LSQ) method, and then to find the direction of the x-axis by adopting the position of Sgr A* at the GC (hereafter the z-fixed method). The second method, called the x-fixed method, fixes the direction the x-axis to the observed position of Sgr A* and then determines the direction of the z-axis with the survey data. In our work, the z-fixed method is modified on the basis of the L11b method (see Sect. 5.1).

3.1 z-fixed Method

The key in the z-fixed method is fitting the x-y plane, which is the basic plane with Galactic stars distributed equally above and below it. To find an optimal position for the basic plane, we divide the sources into 360 bins by Galactic longitude, 1° for each one. Then the sources are re-arranged by the order of their latitudes and the source in the middle of the list is adopted as the median center of the bin. We transform the Galactic coordinate (in the J2000 GalCS) of the median center to the corresponding equatorial coordinate (α, δ), which we can use to fit the position of NGP (i.e. $\alpha^{\rm p}$ and $\delta^{\rm p}$) by applying the LSQ method to the following equation

$$\tan\delta = \sin(\alpha - \alpha_{\rm N}) \cdot \tan i_{\rm N}\,, \tag{2}$$

where $\alpha_{\rm N} = 90^\circ + \alpha^{\rm p}$ is the right ascension of the ascending node and $i_{\rm N} = 90^\circ - \delta^{\rm p}$ is the inclination of the basic plane. We derived Equation (2) from the relative orientation of the Galactic equator and the celestial equator (see fig. 2 in L11b) with the formula for a spherical triangle.

We obtained the position of NGP $(\alpha^{\rm p}, \delta^{\rm p})$, which is the normal vector defining the direction of the basic plane, by iteration. Table 1 lists the positions of the basic planes derived from the z-fixed method with data in different bands.

Table 1 The Positions of Revised x-y Planes at Different Wavelengths

Catalog	band (μm)	$\alpha^{\rm p}$ (°)	$\delta^{\rm p}$ (°)
AKARI	9	192.405 ± 0.137	26.6721 ± 0.0992
	90	192.168 ± 0.133	26.3946 ± 0.0983
WISE	3.4	192.873 ± 0.140	26.9534 ± 0.0999
	4.6	192.624 ± 0.140	27.0388 ± 0.1003
	12	192.325 ± 0.425	27.4891 ± 0.4987
	22	192.572 ± 0.625	27.3931 ± 0.9062

Figure 5 presents our new values for $\alpha^{\rm p}$ and $\delta^{\rm p}$ in six bands, associated with the results from the 2MASS (1.25 μm band) and the SPECFIND v2.0 (radio band) catalogs as provided by L11b. In Figure 5 we find that the results differ significantly among the eight bands. $\alpha^{\rm p}$ and $\delta^{\rm p}$ generally decrease with the increase of wavelength. The differences between the values for both $\alpha^{\rm p}$ and $\delta^{\rm p}$ derived from different bands are on the order of 0.1°.

To define a new GalCS using the above results, we adopt the mean values of $\alpha^{\rm p}$ and $\delta^{\rm p}$ and obtain the position angle θ of the GC with the relationship

$$\tan\theta = \frac{\sin\left(\alpha^0 - \alpha^{\rm p}\right)}{\cos\delta^{\rm p}\tan\delta^0 - \sin\delta^{\rm p}\cos\left(\alpha^0 - \alpha^{\rm p}\right)}\,, \tag{3}$$

where (α^0, δ^0) is the equatorial coordinate of the observational position of the GC (Sgr A*). The values of α^0 and δ^0 can be found in Reid & Brunthaler (2004)

$$\alpha^0 = 17^{\rm h}45^{\rm m}40.0400^{\rm s},\ \delta^0 = -29^\circ00'28.138''\,. \tag{4}$$

In this situation, the zero-point of the GalCS is actually the projected point in the direction of Sgr A*.

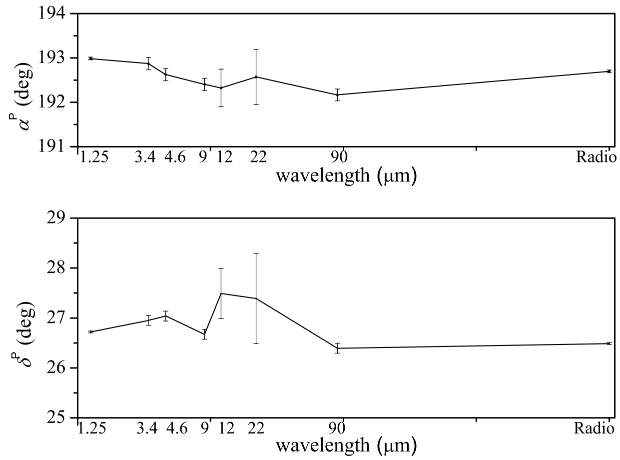

Fig. 5 The values of α^{P} and δ^{P} fitted at different wavelengths with the z-fixed method.

The new parameters (based on the z-fixed method) that define the orientation of the new GalCS in the ICRS are such that

$$\begin{aligned} \alpha^{\mathrm{P}}_{z-\mathrm{fixed}} &= 192.582^\circ\,, \\ \delta^{\mathrm{P}}_{z-\mathrm{fixed}} &= 26.8935^\circ\,, \\ \theta_{z-\mathrm{fixed}} &= 122.86216^\circ\,. \end{aligned} \tag{5}$$

3.2 x-fixed Method

In the x-fixed method, we first fix the direction of the x-axis to the position of Sgr A* in Equation (4), and then determine the z-axis perpendicular to the x-axis using our selected data. In order to find an optimal z-axis, we can fit the position angle η of the NGP (see fig. 5 of L11b) using the equation

$$\cos\delta^0 \tan\delta = \sin\delta^0 \cos\left(\alpha - \alpha^0\right) + \sin\left(\alpha - \alpha^0\right)\tan\eta\,, \tag{6}$$

where (α, δ) is the equatorial coordinate of the geometric center (i.e. a center with the averaged Galactic longitude and latitude of all the sources in a bin) in each bin.

In this calculation, we found that the values of η derived from every bin center differ very much near the GC and the Galactic anticenter (GAC) (see Fig. 6).

$$\begin{aligned} \partial\tan\eta/\partial\alpha &= \frac{\sin\delta^0 - \cos\delta^0\tan\delta\cos(\alpha-\alpha^0)}{\sin^2(\alpha-\alpha^0)} \\ \partial\tan\eta/\partial\delta &= \frac{\cos\delta^0}{\cos^2\delta\sin(\alpha-\alpha^0)}\,. \end{aligned} \tag{7}$$

We can infer from Equation (7) that if the position of the bin-center approaches the GC or the GAC, $\partial\tan\eta/\partial\alpha$ tends to be $\pm\frac{1}{2}\sin\delta^0$ but $\partial\tan\eta/\partial\delta$ will be infinity. So, the GC and GAC are two singular points which can make the values of η very unstable around them. As an example, in Figure 6 large departures are seen, which show the possibility of poor determination of η at the positions of the GC and GAC.

In this case, we discarded abnormal values of η in several bins (depending on the various situations in different bands) near the GC and the GAC, and obtained more reliable results for η in

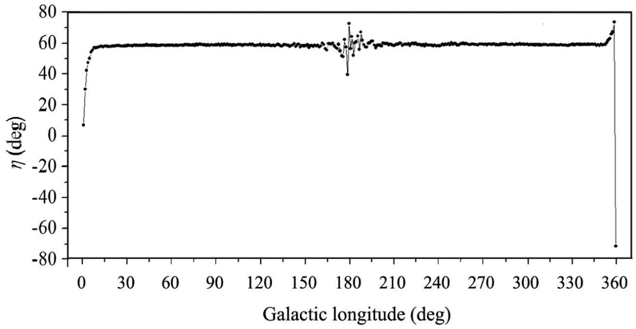

Fig. 6 Values of η derived in 360 bins for 9 μm data from AKARI with Equation (6).

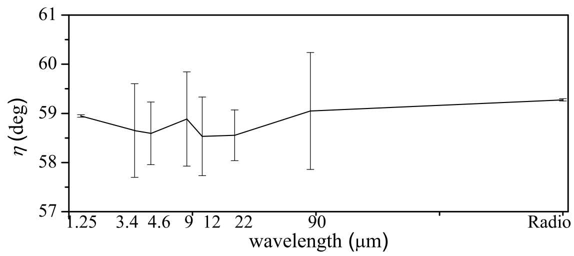

Fig. 7 Values of η fitted in different bands with the x-fixed method.

six wavelengths as shown in Figure 7, associated with values in the 1.25 μm band from the 2MASS survey and the radio band from SPECFIND provided by L11b.

We adopt the mean value of η to characterize the direction of NGP

$$\eta = 58.811^\circ \,. \tag{8}$$

After that we obtain new GalCS parameters by applying this new η and the position of Sgr A* (α^0, δ^0)

$$\begin{aligned} \tan\theta &= \sin\eta / \tan\delta^0 \,, \\ \cos\delta^{\rm p} &= \sin\eta\cos\delta^0 / \sin\theta \,, \\ \sin(\alpha^0 - \alpha^{\rm p}) &= \sin\theta / \cos\delta^0 \,. \end{aligned} \tag{9}$$

The numerical values for the final GalCS parameters are

$$\begin{aligned} \alpha^{\rm p}_{x-\rm fixed} &= 192.777^\circ \,, \\ \delta^{\rm p}_{x-\rm fixed} &= 26.9298^\circ \,, \\ \theta_{x-\rm fixed} &= 122.95017^\circ \,. \end{aligned} \tag{10}$$

4 THE GALACTIC WARP IN DIFFERENT GALCSS

It has been more than half a century since it was found from radio observations that neutral hydrogen revealed the gaseous disk of the Milky Way to be warped (see e.g. Burke 1957, Kerr 1957, Westerhout 1957), like an elongated, oblate, horizontal “S” if we observe it from edge-on. Studying the form of the warp plane is closely related to the GalCS. We can analyze the effect of different GalCSs on the study of the structure of the Milky Way by comparing parameters that fit the warp, the

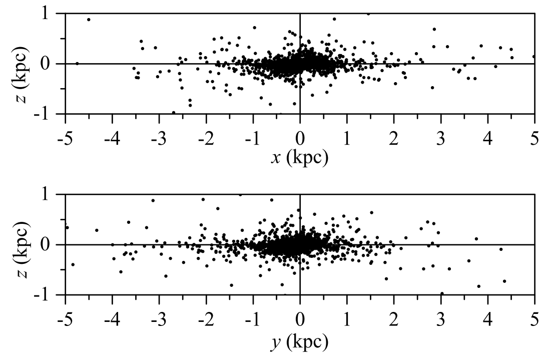

Fig. 8 The projection of warp stars (from Hipparcos O-B5 stars) onto the $x - z$ and $y - z$ planes of the J2000.0 GalCS. The center, denoted by $(0,\ 0)$, represents the Sun.

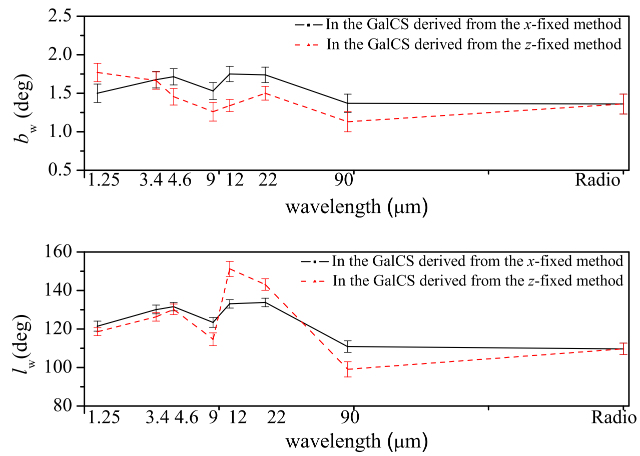

Fig. 9 The warp parameters fitted in the GalCS in eight bands. Results in the GalCS derived from the x-fixed and z-fixed methods at each wavelength are provided for comparison.

inclination angle $b_{\rm w}$ of the warp plane with respect to the Galactic plane and the Galactic longitude $l_{\rm w}$ of the intersection line for the two planes:

$$\cos b_{\rm w} = \frac{|c|}{\sqrt{a^2 + b^2 + c^2}}\,, \qquad \tan l_{\rm w} = -\frac{a}{b}\,, \tag{11}$$

where a, b and c are the coefficients to be determined in the plane equation $ax + by + cz = 1$ (with $x,\ y,\ z$ being the Galactic rectangular coordinates of a star in the warp plane).

The data used to fit the warp plane are from Hipparcos O-B5 stars (Miyamoto & Zhu 1998). After selecting warp stars with proper ages and parallaxes, we obtained a visualized form of the warp (see Fig. 8) and the parameters describing the warp plane using positions and parallaxes of the warp stars. The results (in the GalCS derived from the x-fixed method) are listed in Table 2, and Figure 9 shows the relationship between the warp parameters and wavelengths.

Table 2 The parameters of the Galactic warp in different GalCSs derived from the x-fixed method.

Catalog	GalCS $(\mu\mathrm{m})$	$b_{\mathrm{w}}(^{\circ})$	$l_{\mathrm{w}}(^{\circ})$
2MASS	1.25	1.50 ± 0.12	121.49 ± 2.61
	3.4	1.68 ± 0.11	130.15 ± 2.27
WISE	4.6	1.71 ± 0.11	131.61 ± 2.22
	12	1.75 ± 0.10	133.08 ± 2.16
	22	1.74 ± 0.10	132.58 ± 2.18
AKARI	9	1.53 ± 0.11	123.42 ± 2.55
	90	1.37 ± 0.12	110.91 ± 2.98
SPECFIND	Radio	1.36 ± 0.13	109.64 ± 3.02

Notes: The GalCS related to 2MASS and SPECFIND are from L11b.

In Figure 9, both b_{w} and l_{w} evidently change with the wavelengths. These variations in the warp parameters are the results of using different GalCSs in the calculation. This shows that an explicit and unitive definition of the GalCS is important for studying Galactic structures, especially for modeling substructures which are located close to or inside the Galactic disk.

5 DISCUSSION AND CONCLUSIONS

In this work, we have used data in six bands from AKARI and WISE all-sky surveys to fit GalCS parameters $(\alpha^{\mathrm{p}}, \delta^{\mathrm{p}}, \theta)$ and made a comparison among different results, including results given by L11b derived from 2MASS and SPECFIND data. The variations of the three GalCS parameters with respect to wavelength are shown in Figures 5 and 7. Generally, α^{p} and δ^{p} decrease with an increase of wavelength, but the trend in η is not obvious. Moreover, we have made some improvements to the two methods used for fitting the GalCS parameters based on the L11b paper to refine our results. Finally, we compared the form of the warp in different GalCSs to point out the effect of the GalCS on the study of Galactic structures. In our work, several analyses and problems are discussed in the following subsections.

5.1 A Comparison between the Basic Plane Fitted to Median Centers and the One Fitted to Geometric Centers

The major improvement we made in the z-fixed method is adopting the median centers of 1°-Galactic-longitude bins instead of geometric centers used in L11b to find a more proper basic plane.

We note that the vertical height of the Sun above the Galactic disk is about 15 pc (Zhu 2009), resulting in an effect that every star on the Galactic disk is projected toward the south Galactic pole. However the density of sources near the GC is much higher than that at any other longitudes, so the accumulated southward effect resulting from projection for the geometric bin centers will be non-uniform: the greatest effect can be found at the $l = 0^{\circ}$ bin (the GC). This will distort the projected plane on the celestial sphere. On the other hand, using the median center of each bin enables us to efficiently avoid such bias because it is not an accumulated effect. Therefore, the basic plane derived from median centers is a plane passing through the Sun while staying approximately parallel to the Galactic disk.

In order to make a comparison between the two kinds of basic planes (i.e. derived from geometric or median centers) expressed above, we also use geometric centers to calculate another series of $(\alpha^{\mathrm{p}}, \delta^{\mathrm{p}}, \theta)$ to establish the GalCS in the entire six bands following the LSQ method in Section 3.1. By comparing the positions of Sgr A* in the two kinds of GalCSs, we found that the latitudes of Sgr A* in the GalCS corresponding to median centers are about 0.1° lower than those in the GalCS constructed with geometric centers in almost all the bands, which verifies results of our analysis that the plane fitted to geometric centers is inclined to the south with respect to the plane fitted with median centers in the direction of $l = 0°$. The plane fitted to median centers is almost parallel to the Galactic disk because Sgr A* is $0.13°$ below the basic plane in the final result (listed in Eq. (5)), which coincides with the vertical displacement of the Sun above the Galactic plane (~ 15 pc) (Zhu 2009) and the Galactocentric distance of the Sun (~ 8.0 kpc) (Reid 1993).

From the analyses above, we can conclude that the GalCS established with median centers should be a better system for studying Galactic substructures, especially the structures near the Galactic disk, because the basic plane fitted to median centers is approximately parallel to the Galactic disk.

5.2 Averaging Galactic Parameters Derived from Data in Different Bands

The relationship between Galactic parameters and wavelengths (see Fig. 5 and Fig. 7) highlights the complicated structure of the Milky Way. The Galactic disk contains many different components of sources. These components differ in terms of evolutionary phases, distribution, detected wavelengths, etc. Also, the strength of extinction theoretically becomes weaker when wavelength increases, but the contamination in the survey may become serious at the same time (see Fig. 2 and Fig. 3). We need to analyze the characteristics and quality of data in each band and try to select a quality sample for that band to calculate GalCS parameters. Noting that the precision and reliability of results derived from data in different bands are related to lots of factors and that none of these revised GalCSs is more representative than others, we decided to adopt an equal weight of the result at each wavelength when averaging $\alpha^{\rm p}$, $\delta^{\rm p}$ and η in Section 3. The error bars, shown in Figures 5 and 7, only denote the fitting precisions of data, which are not suitable for determining the weights of different results.

5.3 Comparison between the z-fixed and x-fixed Methods

In this work, we applied two methods to establish a GalCS and the results of the z-fixed and x-fixed methods differ on the order of $0.1°$. From Figure 9 we can see that the difference between the two methods can obviously impact the study of Galactic structure.

Because the vertical position of the Sun is above the Galactic disk, the basic plane derived by the two methods has different geometric interpretations. The advantage of the z-fixed method is reflected in the relatively optimal basic plane that stays almost parallel to the Galactic disk (see Sect. 5.1). However, its disadvantages are more obvious. In this method, the basic plane depends strongly on the distribution of the data. The extinction near the Galactic disk and the contamination in the data can impact the precision of the fitted parameters. Moreover, the uncertainty in the value of the position angle θ of the GC is enlarged because of its dependence on $\alpha^{\rm p}$ and $\delta^{\rm p}$ which have non-negligible fitting errors.

For the x-fixed method, the basic plane is forced to pass through the Sun and Sgr A*, which makes it inclined with respect to the Galactic disk but more practicable in calculations, and the inclination of this basic plane with respect to the Galactic disk (around $0.1°$) is not big enough to seriously impact the study of Galactic structure or kinematics under the current circumstances. Moreover, the number of GalCS parameters derived from multi-wavelength catalogs is only one (the position angle of NGP, η), but in the z-fixed method, two parameters ($\alpha^{\rm p}$ and $\delta^{\rm p}$) depend on the catalogs. In this case, the definition of a GalCS corresponding to the x-fixed method is considered to be more advantageous, although the results are affected by the singular points for calculating η as discussed in Section 3.2.

In fact, the main question is what kind of GalCS we need: a tilted one passing through Sgr A* (corresponding to the x-fixed method) or one staying parallel to the Galactic disk (corresponding to the z-fixed method).

5.4 Recommendation for New GalCS

By comparing the two methods, we note that the x-fixed method can provide us with a more reliable GalCS by considering its lower uncertainty. Therefore, we recommend results derived from the x-fixed method to be the new GalCS parameters, which are summarized in Equation (10). The inclination of the revised basic plane with respect to the original basic plane is $0.2°$. The numerical transformation matrix $\mathcal{N}$ from the equatorial to the GalCS can be written as:

$$\mathcal{N} = \begin{pmatrix} -0.0546533401 & -0.8728440988 & -0.4849290583 \\ +0.4909257965 & -0.4463911532 & +0.7481489161 \\ -0.8694854080 & -0.1971753470 & +0.4528984519 \end{pmatrix} .$$

The transformation matrix $\mathrm{d}\mathcal{N}$ from the J2000.0 GalCS to our new GalCS is:

$$\mathrm{d}\mathcal{N} = \begin{pmatrix} +0.9999992010 & -0.0009712909 & -0.0008090114 \\ +0.0009742004 & +0.9999930322 & +0.0036036810 \\ +0.0008055055 & -0.0036044663 & +0.9999931795 \end{pmatrix} .$$

Although there exist several uncertainties, the newly established GalCS better incorporates features in the Milky Way than the traditional one. The transformation definition based on IAU 1958 GalCS could be dropped and the new definition of the GalCS based on modern observations is possible.

Acknowledgements This work was funded by the National Natural Science Foundation of China under grant Nos. 11173014 and 11473013 and the Natural Science Foundation of Jiangsu Province under grant No. BK20130546. This research is based on observations with AKARI, a JAXA project with the participation of ESA and has made use of the NASA/IPAC Infrared Science Archive, which is operated by the Jet Propulsion Laboratory, California Institute of Technology, under contract with the National Aeronautics and Space Administration.

References

Blaauw, A., Gum, C. S., Pawsey, J. L., & Westerhout, G. 1960, MNRAS, 121, 123
Burke, B. F. 1957, AJ, 62, 90
Ishihara, D., Onaka, T., Kataza, H., et al. 2010, A&A, 514, A1
Kawada, M., Baba, H., Barthel, P. D., et al. 2007, PASJ, 59, 389
Kerr, F. J. 1957, AJ, 62, 93
Liu, J.-C., Zhu, Z., & Hu, B. 2011a, A&A, 536, A102
Liu, J.-C., Zhu, Z., & Zhang, H. 2011b, A&A, 526, A16
Miyamoto, M., Yoshizawa, M., & Suzuki, S. 1988, A&A, 194, 107
Miyamoto, M., & Zhu, Z. 1998, AJ, 115, 1483
Murakami, H., Baba, H., Barthel, P., et al. 2007, PASJ, 59, 369
Murray, C. A. 1989, A&A, 218, 325
Onaka, T., Matsuhara, H., Wada, T., et al. 2007, PASJ, 59, 401
Reid, M. J. 1993, ARA&A, 31, 345
Reid, M. J., & Brunthaler, A. 2004, ApJ, 616, 872
Westerhout, G. 1957, Bull. Astron. Inst. Netherlands, 13, 201
Westin, T. N. G. 1985, A&AS, 60, 99
Wright, E. L., Eisenhardt, P. R. M., Mainzer, A. K., et al. 2010, AJ, 140, 1868
Zhu, Z. 2009, RAA (Research in Astronomy and Astrophysics), 9, 1285